Underfilm corrosion of steel sheets observed by confocal 3D-XRF technique

Koji Akioka,[1,a)] Takashi Nakazawa,[2] Takashi Doi,[1] Masahiro Arai,[1] and Kouichi Tsuji[3]
[1]*Nippon Steel & Sumitomo Metal Corporation 1-8 Fuso-cho, Amagasaki, Hyogo 660-0891, Japan*
[2]*Faculty of Science and Engineering, Chuo University 1-13-27, Kasuga, Bunkyo-ku, Tokyo 112-8551, Japan*
[3]*Graduate School of Engineering, Osaka City University 3-3-138, Sugimoto-cho, Sumiyoshi-ku, Osaka 558-8585, Japan*

(Received 13 March 2014; accepted 14 March 2014)

A confocal micro-X-ray fluorescence (XRF) method with a vacuum chamber was used for investigation of underfilm corrosion that occurs on a painted steel sheet used for automotive applications. A painted steel sheet was prepared by applying electrodeposition coating onto an electro-galvanized steel sheet with a zinc phosphate conversion coating. The spatial resolution of the confocal micro-XRF was about 10.9 ?m at an energy of 17.4 keV. The phosphorus signal from the zinc phosphate layer was able to be observed nondestructively by measuring under the vacuum condition. Each layer of the painted steel sheet was observed from the depth profile analysis of the characteristic elements of each layer. The painted steel sheet was scratched to expose the substrate surface, and then the sheet was then immersed in a NaCl solution for 10 days. The in-depth elemental map of Ti of the corroded steel sheet revealed blister-type corrosion around the scratch. The in-depth elemental maps of Zn and P suggested that the zinc phosphate layer dissolved from the scratched part into the NaCl solution. © *2014 International Centre for Diffraction Data*. [doi:10.1017/S0885715614000293]

Key words: confocal micro-XRF, underfilm corrosion

I. INTRODUCTION

Corrosion is one of the most crucial problems of steel sheets for automotive applications. Corrosion deteriorates not only the appearance of body panels but also the safety of passengers because of the damage in the functioning of the steering or braking system. Most car manufacturers have corrosion warranties for safe driving (Androsch *et al.*, 2001). Usually, zinc coating steel sheets are used to prevent corrosion of the steel sheet. In addition, the steel sheets used for car body panels are painted by electrodeposition coating (e-coating) after the zinc phosphate conversion coating. Thus, one of the corrosion phenomena of the steel sheets used for car body panels is underfilm corrosion. In the case of layered samples, such as painted steel sheets, elemental depth profiles give important information for the estimation of the corrosion mechanism. For this purpose, the corroded sample is usually angle polished, and a cross-sectional image of the sample is analyzed by micro-analysis methods such as scanning electron microscope-energy dispersive X-ray spectrometer (SEM-EDS). Several models of underfilm corrosion have been proposed on the basis of these destructive analyses (Shastry and Townsend, 1989; Hayashi *et al.*, 1990). The proposed mechanism of underfilm corrosion depended on the corrosion condition. The salt spray test, which is conducted in wet condition, was compared with the cyclic corrosion test, which has a dry process (Shastry and Townsend, 1989).

X-ray fluorescence (XRF) is a nondestructive method used to obtain elemental information. It was conventionally used to measure the coating weight of zinc phosphate (Kojima *et al.*, 1980). In the early 1990s, the basic principle of confocal three-dimensional (3D)-XRF was proposed (Gibson and Kumakhov, 1992). By combining with polycapillary X-ray lenses to the X-ray tube and the detector, the analyzing volume was limited. Therefore, a nondestructive depth-selective analysis was achieved. Using this basic principle, the depth profiling was first demonstrated for art-historical objects (Kanngiesser *et al.*, 2003). Tsuji's research group applied this confocal 3D-XRF technique to plant samples (Tsuji and Nakano, 2007; Tsuji *et al.*, 2007), solid/liquid interfaces (Tsuji *et al.*, 2008), Japanese handicraft (Nakano and Tsuji, 2009), and biological samples (Nakano and Tsuji, 2010), using a laboratory-made instrument. Recently, they developed a new confocal 3D-XRF instrument, which has higher depth resolution compared to that of previous instruments using a fine-focus X-ray source and advanced polycapillary optics (Tsuji and Nakano, 2011). The forensic samples such as car paint chips and leather samples were analyzed with this new confocal 3D-XRF instrument (Nakano *et al.*, 2011). In addition, Tsuji's research group developed the advanced setup of a confocal 3D-XRF with a vacuum chamber (Nakazawa and Tsuji, 2013). In this study, this confocal 3D-XRF method with a vacuum chamber was used for investigation of underfilm corrosion phenomena. To discriminate each layer of the painted steel sheet, the depth elemental profiling analysis was performed. And in-depth elemental maps of the characteristic elements of each layer were analyzed to estimate the underfilm corrosion process.

II. EXPERIMENTAL

A. Confocal 3D-XRF system

Two polycapillary X-ray focus optics were used [designed and manufactured by X-Ray Optical Systems Inc.

[a)]Author to whom correspondence should be addressed. Electronic mail: akioka.b9m.kohji@jp.nssmc.com

(XOS), USA]. The primary X-ray from a metal ceramic-type 50 W X-ray tube with an Rh anode (MCBM 50-0.6B, 50 kV and 0.5 mA, rtw, Germany) was focused by a polycapillary X-ray full lens. The focal spot size was experimentally evaluated to be 10 μm at an X-ray energy of 17.4 keV (Mo$K\alpha$) by XOS. Another polycapillary half lens was attached to a silicon drift X-ray detector (Vortex EX-60, SII Nano Technology Inc., USA) [sensitive area: 50 mm^2, energy resolution <130 eV at 5.9 keV (Mn$K\mu$)]. A sheet sample was set horizontally on an X–Y–Z stage (XA04A-R2-1J and ZA07A-R3S-2H, Kohzu Precision Co., Ltd., Japan). To achieve the optimum confocal geometry with the incident and detection beams, both polycapillary X-ray lenses were set at an angle of 45° to the vertical axis. The 3D-XRF measurement was performed by scanning the confocal point in vacuum under 1×10^{-2} Torr. The depth resolution of the confocal 3D-XRF instrument evaluated by a thin-film scanning method was 56 μm at an energy of 1.49 keV (Al$K\alpha$) and 10.9 μm at 17.4 keV (Mo$K\mu$) (Nakazawa and Tsuji, 2013).

B. Painted steel sheet

Mild steel sheet with electro-galvanized coating was used for the analysis. The thickness of the steel sheet was 0.7 mm. The coating weight of the zinc layer was about 60 g m^{-2} at each surface. After the degreasing treatment, conventional tri-cation-type zinc phosphate conversion coating was applied, followed by a cation-type e-coating. After that, the painted steel sheet was baked in a drying oven at 170 °C. The cross-sectional back-scattered electron detector (BSE) image of the polished resin-embedded sample is shown in Figure 1. The thickness of the e-coating layer was about 15 μm. The zinc phosphate conversion coating existed in the interface of the e-coating and the zinc coating. The zinc coating layer, which observed brighter than the steel substrate, was about 8 μm thick.

C. Corrosion condition

A test specimen measuring 35 × 40 mm was cut out of the painted steel sheet. All edges of test specimen were masked with a polyester-insulating tape. The surface of the painted layer was scratched to a length of 15 mm to expose the steel substrate. A dipping-type corrosion test was performed. Sodium chloride solution of concentration 5 wt% was used. The test specimen with the scratch was immersed in a NaCl solution at 55 °C. The test specimen was taken out to observe appearance every 48 h. The test period was 240 h in total. After rinsing with water, the corroded test specimen was dried in a vacuum desiccator. Thereafter, the in-depth elemental analysis was performed by the confocal 3D-XRF in vacuum.

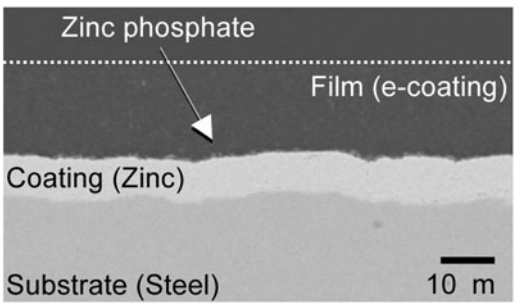

Figure 1. Cross-sectional BSE image of painted steel sheet with zinc coating.

III. RESULTS AND DISCUSSION

A. Elemental depth profiles of painted steel sheet

Elemental depth profiles were obtained by scanning in the depth direction at a fixed position at intervals of 4 μm. The measuring time was 300 s at each analyzed point. The sum spectrum is shown in Figure 2. The peaks corresponding to Fe, Zn, and Ti were clearly observed from the steel substrate, the zinc coating, and pigment of the paint film, respectively. Sum peaks of Fe and Zn were observed at the higher energy region. Mn and Ni peaks were considered from the tri-cation component of the zinc phosphate coating. L lines of Sn signal were considered from anti-corrosion pigment of the e-coating. L lines of Rh signal originated from the X-ray tube. The phosphorous signal from the zinc phosphate layer was observed by measuring under vacuum condition. In addition, the signals of Al and Si, which were components of paint pigment, were clearly observed at the lower energy region.

The elemental depth profile of the painted steel sheet is shown in Figure 3. The *X*-axis corresponds to the scanned distance in the depth direction from the surface (around zero) into the depth. *Y*-axis is the normalized elemental signal. The elemental depth profiling provides the detailed information on the elemental distribution in depth. The profile of each element had a peak, which position in depth corresponded

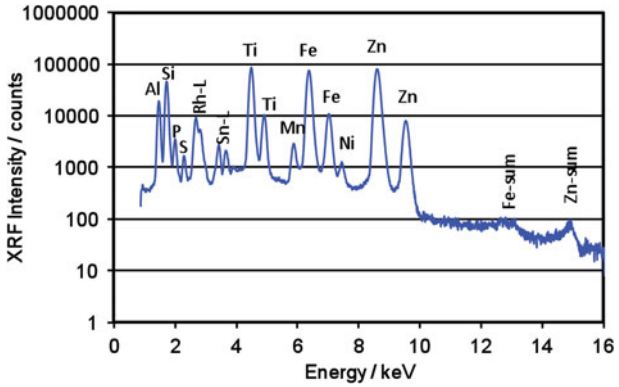

Figure 2. (Color online) Sum spectrum of elemental depth profile of painted steel sheet obtained by confocal 3D-XRF.

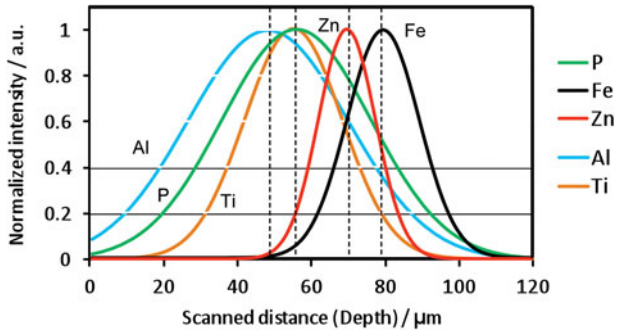

Figure 3. (Color online) Elemental depth profiles of the painted steel sheet. *X*-axis corresponds to scanned distance in the depth direction from the surface.

https://doi.org/10.1017/S0885715614000293 Published online by Cambridge University Press

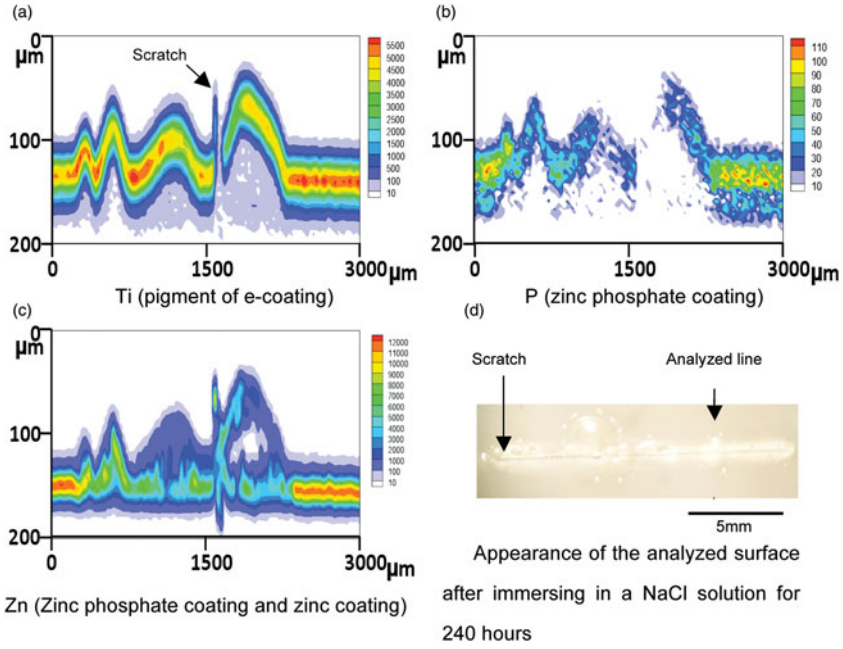

Figure 4. (Color online) In-depth elemental maps of the corroded steel sheet as obtained by confocal 3D-XRF in vacuum for Ti (a), P (b), and Zn (c). The optical microscopic image of the analyzed surface (d) which was immersed in a NaCl solution for 240 h.

to the layer position where element existed. Because the signals decreased for deeper analytical area, the profile of Fe had a peak as other elements. The width of the profile of each element changed corresponding to the depth resolution. In our experimental setup, the depth resolution of Al (56 μm) and P (51 μm) were larger than those of Ti (30 μm) and Zn (18 μm). For this reason, the width of the profile of Al and P were larger than those of Ti and Zn. The distance between Fe and Zn peaks was about 8 μm, which corresponded to the thickness of the zinc-coating layer. The distance between Zn and Ti peaks was about 15 μm, which corresponded to the thickness of the e-coating. On the other hand, the peak of the depth profile of Al positioned near the surface. Therefore, the distance between Zn and Al peaks was about 20 μm, which was wider than those of Zn and Ti. Because of Al and Ti components of pigments of the e-coating, both elements were considered to exist in the same position. The reason for the difference in the peak distance is considered by the effect of the self-absorption. The energy of fluorescence X-rays of Al is smaller than that of Ti, therefore the Al signal from deeper analytical area much decreased than that of Ti. As a result the peak position of Al profile was shifted to outer position. According to the above analyses, the elemental depth profiles showed the elemental position and the thickness of each layer.

B. In-depth elemental maps of the corroded painted steel sheet

In-depth elemental maps of the corroded steel sheet were measured nondestructively using the confocal 3D-XRF analysis in vacuum. The step size was 30 μm in the horizontal direction and 4 μm in the depth direction. The mapping area was 3000 μm in the horizontal direction and 160 μm in the depth direction. The measurement time was 10 s at each analyzed point. In-depth elemental maps of the corroded steel sheet are shown in Figure 4.

X-axis corresponds to the scanned distance in parallel with the painted surface. And the *Y*-axis corresponds to the scanned distance in the depth direction. Color contour indicates the obtained intensity of each element. Figures 4(a)–4(c) represent in-depth elemental maps of Ti (pigment of the e-coating), P (zinc phosphate coating), and Zn (zinc phosphate coating and zinc coating), respectively. The position at which the surface was scratched is indicated in Figure 4(a). The appearance of the analyzed surface of the corroded steel sheet is shown in Figure 4(d). In the region from 2500 to 3000 μm in the *Y*-axis, where any corrosion occurred, the elemental maps of Ti, P, and Zn showed almost flat profile. On the other hand, in other region where corrosion occurred, the elemental map of Ti showed wavy profile around the scratched position. It corresponded to the blister-type corrosion. The intensities of P and Zn decreased at the region where the corrosion blisters occurred. These results indicate that the zinc phosphate layer and zinc coating layer dissolved in the NaCl solution, and then, the blisters of the e-coating occurred. Therefore, the confocal 3D-XRF method nondestructively revealed the blister-type corrosion beneath the paint layer.

IV. CONCLUSIONS

A confocal 3D-XRF method, combined with two individual polycapillary lenses in vacuum, was applied to nondestructively observe the underfilm corrosion of the painted steel sheet. With the improvement in the sensitivity of detection of light elements by measuring in vacuum, we obtained the phosphorus signal from the zinc phosphate layer nondestructively. The spatial resolution of the confocal 3D-XRF was about 10.9 μm at an energy of 17.4 keV, which was sufficient to distinguish between each layer of the painted steel sheet. The blister-type corrosion around the scratch was observed by analyzing the in-depth elemental maps. The in-depth elemental maps of Zn and P indicated that some Zn and P atoms in the zinc phosphate layer dissolved from the scratched part into the NaCl solution. We successfully observed nondestructively the underfilm corrosion of the painted steel sheet by measuring the in-depth elemental maps with the confocal 3D-XRF in vacuum. The results

https://doi.org/10.1017/S0885715614000293 Published online by Cambridge University Press

obtained in this study indicate a great advantage of a confocal micro-XRF analysis for analyzing underfilm corrosion process.

ACKNOWLEDGEMENTS

This work was supported by a Japan Society for the Promotion of Science (JSPS) Grant-in-Aid for Scientific Research (B) and The Iron and Steel Institute of Japan (ISIJ) Research Promotion Grant.

Androsch, F. M., Kosters, K., and Stellnberger, K-H. (**2001**). "Accelerated corrosion tests for corrosion protection systems on steel sheet for the automotive industry," stahl eisen, **121**, 37–46

Gibson, W. M. and Kumakhov, M. A. (**1992**). "Application of X-ray and neutron optics," Proc. SPIE. **1736**, 172–189.

Hayashi, K., Ito, Y., Kato, C., and Miyoshi, Y. (**1990**). "Under-film corrosion behavior of zinc and zinc alloy coated steel sheets for automobiles," Tetsu-to-hagane, **76**, 1317–1324.

Kanngiesser, B., Malzer, W., Reiche, I. (**2003**). "A new 3D micro X-ray fluorescence analysis set-up – first archaeometric applications," Nucl. Instrum. Method Phys. Res. B **211**, 259–264.

Kojima, R., Okita, H., and Matsushima, Y. (**1980**). "Fundamental characteristics of zinc phosphate coating," Tetsu-to-hagane, **66**, 924–934.

Nakano, K. and Tsuji, K. (**2009**). "Nondestructive elemental depth profiling of Japanese lacquerware 'Tamamushi-nuri' by confocal 3D X-ray analysis in comparison with micro GE-XRF," X-Ray Spectrom. **38**, 446–450.

Nakano, K. and Tsuji, K. (**2010**). "Development of laboratory confocal 3D-XRF spectrometer and nondestructive depth profiling," J. Anal. At. Spectrom. **25**, 562–569.

Nakano, K., Nishi, C., Otsuki, K., Nishiwaki, Y., and Tsuji, K. (**2011**). "Depth elemental imaging of forensic samples by confocal micro-XRF method," Anal. Chem. **83**, 3477–3483.

Nakazawa, T. and Tsuji, K. (**2013**). "Development of a high resolution confocal micro-XRF instrument equipped with a vacuum chamber," X-Ray Spectrom. **42**, 374–379.

Shastry, C. R. and Townsend, H. E. (**1989**). "Mechanisms of cosmetic corrosion in painted zinc and zinc-alloy-coated sheet steels," Corrosion, **45**, 103–119.

Tsuji, K. and Nakano, K. (**2007**). "Development of confocal 3D micro XRF spectrometer with Cr–Mo dual excitation," X-Ray Spectrom. **36**, 145–149.

Tsuji, K. and Nakano, K. (**2011**). "Development of a new confocal 3D-XRF instrument with an X-ray tube," J. Anal. At. Spectrom. **26**, 305–309.

Tsuji, K., Nakano, K., and Ding, X. (**2007**). "Development of confocal micro X-ray fluorescence instrument using two X-ray beams," Spectrochim. Acta Part B **62**, 549–553.

Tsuji, K., Yonehara, T., and Nakano, K. (**2008**). "Application of confocal 3D micro-XRF for solid/liquid interface analysis," Anal. Sci. **24**, 99–103.